Journal of Electrical Engineering & Technology (2022) 17:319–328
https://doi.org/10.1007/s42835-021-00865-8

ORIGINAL ARTICLE

Study on Performance Parameters of Short-Secondary Type Slotless Permanent Magnet Linear Synchronous Motor Based on Analytic Method

Hao Liu[1] · **Xiaoju Yin**[2]

Received: 19 January 2021 / Revised: 23 April 2021 / Accepted: 29 July 2021 / Published online: 9 August 2021

Abstract
This paper mainly studies two-dimensional analytic method to analyze and calculate a short-secondary type slotless permanent magnet linear synchronous motor (SST-SPMLSM) performance. Due to the large air-gap and more magnetic flux leakage of electric machine, this paper proposes the groove-by-groove method to analyze the winding equivalent current density. Meanwhile, the volume current density is used to equivalent the permanent magnet magnetization, which is obtained the permanent magnet equivalent current density. According to the electric machine structure, the divided layers model of the SST-SPMLSM is built. Based on the hierarchical analytical model and equivalent current density of the electric machine, the two-dimensional magnetic vector potential of each region in the SST-SPMLSM is derived by the separated variable method. Combined with the boundary conditions of the electric machine, the magnetic flux densities of the SST-SPMLSM with different regions are derived. In the meantime, a 30 N SST-SPMLSM is designed. On this basis, the magnetic flux density, detent force, and electromagnetic thrust force of the SST-SPMLSM are analyzed and calculated, which of the results are verified by finite element method. From the results, it satisfies the design requirements of the SST-SPMLSM, and verifies the validity and correctness of analytical method.

Keywords Performance analysis · Analytic method · Finite element method · Permanent magnet linear synchronous motor · Slotless motor

1 Introduction

There are slot and slotless for two permanent magnet linear synchronous motors (PMLSMs). The PMLSM with slotted has disadvantages of high thrust force fluctuation, low control accuracy and high detent force [1–4]. Therefore, it hinders the application of the PMLSM in high precision servo system.

Slotless PMLSM (SPMLSM) has advantages of slotless, simple structure, simple winding insertion, low detent force, high slot full ratio, reduced end winding, low noise, low magnetic saturation, low loss, and high control precision [5–7]. Therefore, the SPMLSM attracts research of many research structures and experts. Meanwhile, the SPMLSM has widely used in many fields, for instance transport systems [8], and servo system [9].

At present, some theories have been studied on the SPMLSM. Reference [5] mainly studies reduction of thrust force in SPMLSM to change magnet pole shape. The finite element method (FEM) is used to analyze and calculate back electromotive force of SPMLSM with different magnet pole shapes, which of the results are verified by experiment testing. Reference [7] mainly illustrates design slotless-type permanent magnet linear brushless motor. Meanwhile, the equivalent magnetizing current method is used to analyze and calculated steady-state performance parameters of the slotless-type permanent magnet linear brushless motor. Reference [10] mainly adopts the two-dimensional analytic method is used to analyze and calculate the performance parameters of the slotless double-sided inner armature linear permanent magnet synchronous motor, which of the results are compared with that of zero-dimensional analytic method.

✉ Hao Liu
liuhao368368@163.com

[1] School of Electrical and Control Engineering, Henan University of Urban Construction, Pingdingshan, China

[2] Department of Renewable Energy, Shenyang Institute of Engineering, Shenyang, China

Reference [11] mainly investigates the design principles and detent force analysis of a phase-shift modular slotless tubular PMLSM with three sectional primaries. Reference [12] mainly introduces analytical calculation of back electromotive force (EMF) for linear permanent magnet motors with slotted structure, and considered the effect of slotting. Meanwhile, the linear permanent magnet motors with slotless structure is used the magnetic field effective values and winding factor theories to evaluate the back EMF. These studies are only a part of theoretical research, which needs further study. The paper proposes the analytic method (AM) to analyze the performance parameters of short-secondary type SPMLSM (SST-SPMLSM).

The paper mainly studies on two-dimensional analytic method to analyze and calculate the performance parameters of the SST-SPMLSM. Firstly, due to the large air-gap and more magnetic flux leakage of the SST-SPMLSM, the equivalent current density (ECD) of the permanent magnet and primary winding are considered according to the actual situation, respectively. Meanwhile, according to the electric machine structure and working principles, the hierarchical analytical model of the SST-SPMLSM is built. The solution regions are divided into air, primary yoke, primary winding, air-gap, permanent magnet and secondary yoke. Then, under permanent magnet or primary winding excitation, magnetic vector potential is regarded as variable to deduce the two-dimensional magnetic flux density of the SST-SPMLSM with different regions. In the meantime, a 30 N SST-SPMLSM is designed. At last, the air-gap magnetic flux density, electromagnetic thrust force, and detent force of SST-SPMLSM, which are calculated and analyzed based on two-dimensional analytic magnetic flux density and design dimensions of electric machine. Meanwhile, the results are verified by the FEM.

2 Working Principle and Structure

2.1 Working Principle

The working principle of SPMLSM is similar to that of the traditional permanent magnet synchronous motor and PMLSM, which of construction is illustrated in Fig. 1. The SPMLSM is composed of primary and secondary. The primary is consisted of primary yoke and primary winding. The primary can move or standstill. The primary winding adopts concentrated winding, which acts together with the secondary permanent magnet to generate magnetic field and realize electromechanical energy conversion. The combination of the secondary permanent magnet and the secondary yoke is called the secondary. The secondary may also move or standstill.

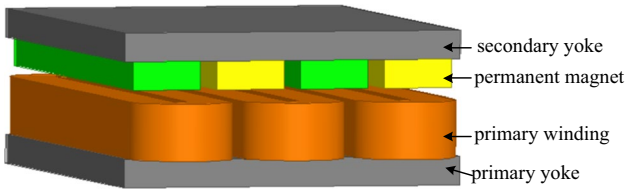

Fig. 1 SPMLSM construction

Three-phase sinusoidal current is fed into the primary winding to generate a traveling wave magnetic field in the air-gap. The electromagnetic thrust force of electrical machine is generated by the interaction of the travelling wave magnetic field and the excitation magnetic field of permanent magnet. Under the action of electromagnetic thrust force, the SPMLSM secondary would move in a straight line in the opposite direction of the travelling wave magnetic field because the electrical machine primary is stationary. Otherwise, the electrical machine primary moves in the opposite direction because the electrical machine secondary is stationary. If the phase sequence of three-phase sinusoidal current of the SPMLSM is changed, the direction of the travelling wave magnetic field in the SPMLSM can be changed, thereby changing the moving direction of the electric machine secondary. The movement speed of the SPMLSM is expressed

$$\upsilon = 2\tau f \tag{1}$$

where υ expresses the electric machine movement speed, f expresses power frequency, and τ expresses pole pitch.

2.2 Topology Structure

There are the flat and the tubular according to structure type of the SPMLSM. Meanwhile, the flat-type SPMLSMs have the single-sided and the doubly-sided according to the SPMLSM structure. The single-sided SPMLSMs have the long primary short secondary (LPSS) and short primary long secondary (SPLS) according to the movement form of electric machine, which of structures are displayed in Fig. 2. The SPMLSM with SPLS structure has disadvantage of high cost and larger amount of permanent magnet. However, the SPMLSM with LPSS structure has disadvantage of low efficiency and high copper loss. Combined with the technical requirements and actual situation of design electrical machine, this paper selects SPMLSM with LPSS structure, namely short-secondary type slotless permanent magnet linear synchronous motor (SST-SPMLSM).

The SST-SPMLSM primary winding is used the concentrated winding. These windings aren't overlapped. The electric machine model is composed of many models, one

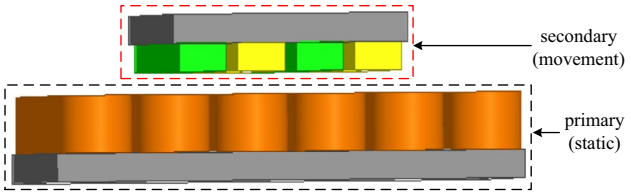

(a) Long primary short secondary

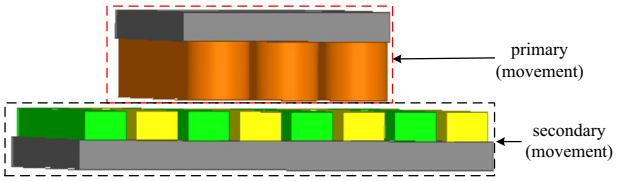

(b) Short primary long secondary

Fig. 2 Single-sided SPMLSM construction

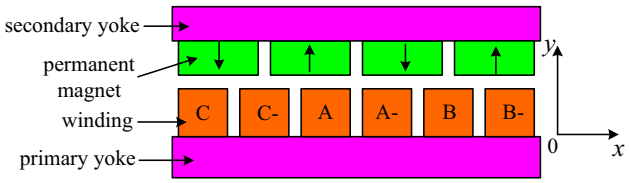

Fig. 3 Four poles and three windings

of which is composed of four poles and three windings, as shown in Fig. 3

3 Magnetic Field Analysis and Examples

This section focuses on magnetic field related issues of electric machine, including PM and winding ECD, analytical model, and analytical magnetic field.

3.1 Equivalent Current Density

3.1.1 Winding Equivalent Current Density

Due to the iron core disconnection and the winding unbalanced distribution of the SST-SPMLSM, the groove-by-groove method is used to calculate and analyze the winding ECD according to the winding actual distribution, which is indicated in Fig. 4. The winding ECD is expressed

$$J_s(x) = \sum_{n=1}^{\infty} b_n \sin\left(\frac{n\pi}{2\tau}x\right) \tag{2}$$

where

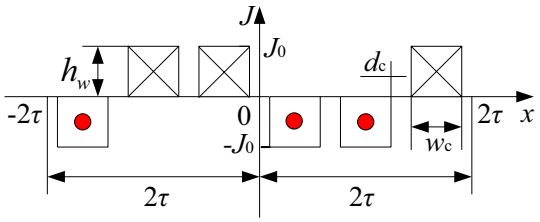

Fig. 4 Winding ECD distribution

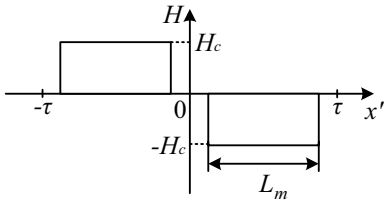

Fig. 5 PM magnetization distribution

$$b_n = -\frac{4}{n\pi}\frac{\sqrt{2}I_1N_s}{w_c h_c}\left[1-\cos\left(\frac{2}{3}n\pi\right)\right] \cdot \sin\left[\frac{n\pi(d_c+w_c)}{4\tau}\right]\sin\left(\frac{n\pi w_c}{4\tau}\right) \tag{3}$$

where w_c expresses winding width, h_w expresses winding height, I_1 expresses phase current, N_s expresses slot number of conductor, d_c expresses distance between two windings, τ expresses pole pitch, J_0 expresses current density.

3.1.2 PM Equivalent Current Density

The volume current density is used to equivalent the PM magnetization, which is shown in Fig. 5. According to the actual distribution, the PM ECD is calculated as follows

$$J_m(x') = \frac{dH}{dx'} \tag{4}$$

where

$$H = \sum_{n=1,3}^{\infty}(-1)^{\frac{n+3}{2}}\frac{4H_c}{n\pi}\cos\left[\frac{n\pi}{\tau}\left(\frac{L_m}{2}-x\right)\right] \tag{5}$$

$$J_m(x') = \sum_{n=1,3}^{\infty}(-1)^{\frac{n+3}{2}}\frac{4H_c}{\tau}\sin\left[\frac{n\pi}{\tau}\left(\frac{L_m}{2}-x'\right)\right] \tag{6}$$

where H_c expresses residual coercive force, and L_m expresses PM longitudinal length.

$$x = x' + x_0 + vt \tag{7}$$

where x_0 expresses mover starting position.

3.2 Analytical Model

In order to establish a suitable magnetic field analysis model for the SST-SPMLSM, the following assumptions of electric machine are made [13, 14]:

(a) Ignoring the change of magnetic field in the direction of z-axis, the current flows only in the direction of z-axis. Based on above the reasons, the magnetic vector potential only has z-direction components. Therefore, the magnetic field can be treated in two dimensions.
(b) According to the actual situation, the groove-by-groove method and the volume current density method are used to calculate the winding and PM current densities, respectively.
(c) The PMs have the same permeability in all direction, which is equal to the air-gap permeability.
(d) The permeability of the primary and secondary yoke is isotropic, which is μ_1 and μ_2, respectively.
(e) The ferromagnetic material is unsaturated.

Based on the SST-SPMLSM assumption, the solving region of electric machine is divided into seven parts, for instance primary exterior region (1, $-\infty \le y \le -h_{j1}$), primary yoke (2, $-h_{j1} \le y \le 0$), primary winding (3, $0 \le y \le a_1$), air-gap (4, $a_1 \le y \le a$), PM (5, $a \le y \le a+b$), secondary yoke (6, $a+b \le y \le a+b+h_{j2}$), and secondary exterior region (7, $a+b+h_{j2} \le y \le \infty$), which is illustrated in Fig. 6.

3.3 Analytical Magnetic Field

Base on the analytical model and structure of the electric machine, the SST-SPMLSM magnetic field is analyzed and calculated to use the separated variable method.

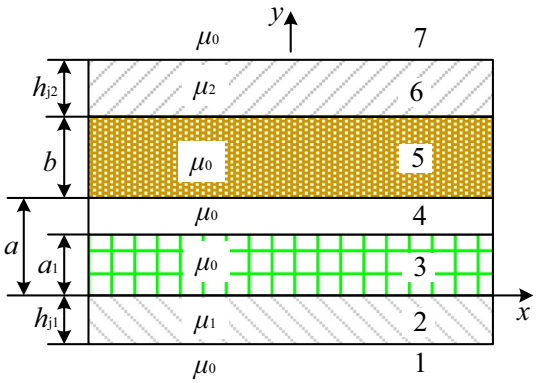

Fig. 6 SST-SPMLSM hierarchical analytical model

The magnetic vector potential equation of magnetic field in the electric machine is as follows [14]

$$\nabla \times \vec{H} = \nabla \times \left(\frac{\vec{B}}{\mu}\right) = \nabla \times \left(\frac{1}{\mu}(\nabla \times \vec{A})\right) \tag{8}$$

where H expresses magnetic field intensity, B expresses magnetic flux density, μ expresses permeability, and A expresses magnetic vector potential.

According to the assumption and ECD of SST-SPMLSM, the magnetic vector potential equation of electric machine is obtained as follows

$$\frac{\partial^2 A_z}{\partial x^2} + \frac{\partial^2 A_z}{\partial y^2} = -\mu_0 J_z \tag{9}$$

where A_z expresses z-direction components of magnetic vector potential, μ_0 expresses air-gap permeability, and J_z expresses current density. In the current region, J_z is not equal to zero, otherwise, it is equal to zero.

The formula (9) is deduced and calculated by the separated variable method, which the results are expressed

$$\begin{aligned} A = &\sum_{n=1}^{\infty} [A_n \cosh(k_n y) + B_n \sinh(k_n y)] \\ &\cdot [C_n \cos(k_n x) + D_n \sin(k_n x)] + \mu_0 \frac{1}{k_n^2} J(x) \end{aligned} \tag{10}$$

where A_n, B_n, C_n, D_n express unknown number, respectively.

When the winding is alone action, the magnetic vector potential of each region in the SST-SPMLSM is calculated and deduced according to the magnetic vector potential equation and hierarchical analytical model, which of results are expressed as follows

$$\begin{aligned} A_i = &\sum_{n=1}^{\infty} [A_n^i \cosh(k_n y) + B_n^i \sinh(k_n y)] \\ &\cdot [C_n^i \cos(k_n x) + D_n^i \sin(k_n x)] \\ &+ \mu_0 \frac{1}{k_n^2} J^i(x) \end{aligned} \tag{11}$$

where i expresses 1, 2, 3, 4, 5, 6, 7, respectively, and A_n^i, B_n^i, C_n^i, D_n^i express unknown number, respectively. When i expresses 3th region,

$$J^3(x) = J_s(x) \tag{12}$$

In addition to 3th region, the current density of other regions is equal to zero.

When the winding is alone action, the air-gap and PM region are considered to have the same magnetic vector potential equation because of the unconsidered permanent magnet. Therefore,

$$A_4 = A_5 \tag{13}$$

The boundary conditions between adjacent regions in the SST-SPMLSM are expressed as follows

$$A_{i+1}\Big|_{y=Y} = A_i\Big|_{y=Y} \tag{14}$$

where Y expresses the height between adjacent regions in a rectangular coordinate system.

In addition to the above boundary conditions, the boundary conditions between adjacent regions in the same permeability region are also expressed as follows

$$\frac{\partial A_{i+1}}{\partial y}\bigg|_{y=Y} = \frac{\partial A_i}{\partial y}\bigg|_{y=Y} \tag{15}$$

In the region with the different permeability, the boundary conditions between regions in the SST-SPMLSM are also expressed as follows

$$\frac{1}{\mu_{i+1}}\frac{\partial A_{i+1}}{\partial y}\bigg|_{y=Y} = \frac{1}{\mu_i}\frac{\partial A_i}{\partial y}\bigg|_{y=Y} \tag{16}$$

The magnetic vector potential of primary and secondary exterior regions in the SST-SPMLSM is zero, which is expressed as follows

$$A_1\big|_{y=-\infty} = A_7\big|_{y=\infty} = 0 \tag{17}$$

Substituting the formula (12)–(17) into formula (11), the undetermined coefficients are solved through derivation and calculation, and the magnetic vector potential of each region in the SST-SPMLSM is obtained. Then, according to relate the magnetic vector potential with magnetic flux density, the magnetic flux density of each region in the electric machine is derived, which is expressed as follows

$$\begin{cases} B_{ix}^W = \partial A_i / \partial y \\ B_{iy}^W = -\partial A_i / \partial x \end{cases} \tag{18}$$

whereB_{ix}^W and B_{iy}^W express x-direction (tangential) and y-direction (radial) magnetic flux density of the electric machine under the winding alone action, respectively.

Based on the magnetic vector potential equation and boundary conditions, the air-gap magnetic flux density of the SST-SPMLSM under the winding alone action, which is derived as follows

$$\begin{aligned} B_{4x}^W = -\mu_0 \sum_{n=1}^{\infty} T_5\{\cosh[k_n(a+b-y)] + T_1 \\ \cdot \sinh[k_n(a+b-y)]\} \cdot \frac{b_n}{k_n}\sin(k_n x) \end{aligned} \tag{19}$$

$$\begin{aligned} B_{4y}^W = \mu_0 \sum_{n=1,3}^{\infty} T_5\{\sinh[k_n(a+b-y)] + T_1 \\ \cdot \cosh[k_n(a+b-y)]\} \cdot \frac{b_n}{k_n}\cos(k_n x) \end{aligned} \tag{20}$$

where B_{4x}^W and B_{4y}^W express the tangential and radial magnetic flux density of air-gap under the winding alone action in the SST-SPMLSM, respectively, T_1 and T_2 express coefficient, respectively, and a and b is expressed

$$\begin{cases} a = h_w + \delta \\ b = h_m \end{cases} \tag{21}$$

where h_{m} expresses the PM magnetization height, and δ expresses the air-gap length.

The method for solving the magnetic density of other regions of the electric machine is similar to that for solving the air-gap region, so the derivation is not given.

Based on above the analytical method, the air-gap magnetic flux density of the SST-SPMLSM is analyzed and calculated under the winding alone action, which of results is displayed in Fig. 7. Under the same electric machine structure and excitation conditions, the FEM is used to analyze and calculate the air-gap magnetic flux density of the SST-SPMLSM, and compared with the analytical results, which is shown in Fig. 7. It is found that the air-gap magnetic flux density curve of the SST-SPMLSM in winding single action for the AM is basically the same with that of the FEM. Meanwhile, the tangential maximum air-gap magnetic flux density and radial maximum air-gap magnetic flux density of the electric machine in winding single action for the AM is 0.30% and 0.98% lesser than that of the FEM, respectively.

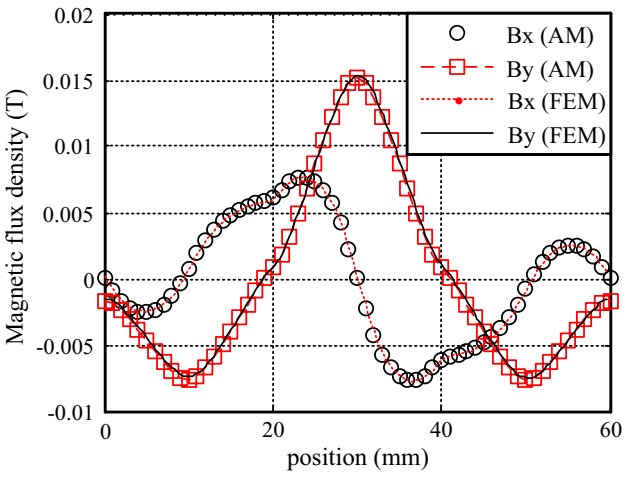

Fig. 7 Air-gap magnetic flux density of SST-SPMLSM in winding single action

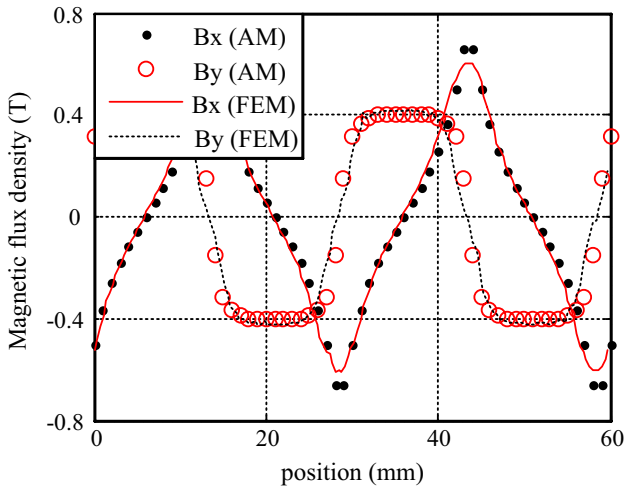

Fig. 8 Air-gap magnetic flux density of SST-SPMLSM in PM single action

As for the magnetic vector potential of each region of the SST-SPMLSM in the PM single action, its solution process is similar to that of the winding alone action, so it will not be repeated here. On this basis, the air-gap magnetic flux density of the electric machine for the PM alone action is analyzed and calculated, which is verified by the FEM, and the results are shown in Fig. 8. It is found that the air-gap magnetic flux density curve of the SST-SPMLSM in PM single action for AM is basically the same with that of the FEM. Meanwhile, the tangential maximum air-gap magnetic flux density of electric machine in the PM single action for the AM is 8.89% higher than that of the FEM. However, the radial maximum air-gap magnetic flux density of the electric machine in PM single action for the AM is 4.46% lesser than that of the FEM.

The magnetic flux density of each region in the SST-SPMLSM is the sum of the magnetic flux density of each region under the winding alone action and the magnetic flux density of each region under the PM alone action, which is expressed as follow

$$\begin{cases} B_{xi} = B_{xi}^{M} + B_{xi}^{W} \\ B_{yi} = B_{yi}^{M} + B_{yi}^{W} \end{cases} \tag{22}$$

where B_{xi}^{M},B_{yi}^{M} express the tangential and radial magnetic flux density of the electric machine in the PM single action, respectively, and B_{xi},B_{yi} express the tangential and radial of each region in the SST-SPMLSM, respectively.

4 Modes Design SST-SPMLSM

Based on design principle and method of the electric machine, the design flow chart and main parameters of the SST-SPMLSM are displayed in Fig. 9 and Table 1.

5 Parameters Analysis and Verification

This section mainly discusses and analyzes the performance parameters of the SST-SPMLSM, including magnetic flux density, detent force, electromagnetic thrust force and vertical force.

5.1 Magnetic Flux Density

Based on the main dimensions of the design SST-SPMLSM, the AM is used to analyze and calculate the magnetic flux density of electric machine, which of the results are illustrated in Fig. 10. It is found that the AM is used to solve the air-gap and winding surface magnetic flux density curves of the SST-SPMLSM are basically the same with that of the FEM, which of the results are verified the correctness and effectiveness of analytical method. Meanwhile, the AM is used to calculate the air-gap and winding surface maximum

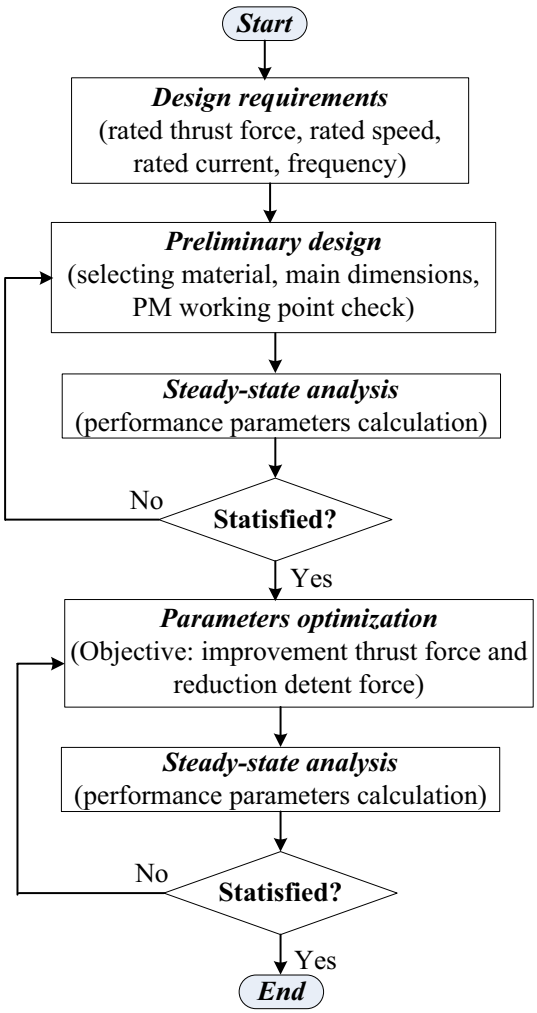

Fig. 9 Design flow chart of SST-SPMLSM

Table 1 Main parameters of design SST-SPMLSM

Parameter	Number
Rated thrust force (N)	30
Rated speed (mm/s)	180
Rated current (A)	3.75
Rated frequency (Hz)	6
Number of pole pairs	6
Pole pitch (mm)	15
Air-gap (mm)	2
PM magnetization height (mm)	5
PM longitudinal length (mm)	12
Conductors per slot	50
Primary yoke height (mm)	5
Secondary yoke height (mm)	5

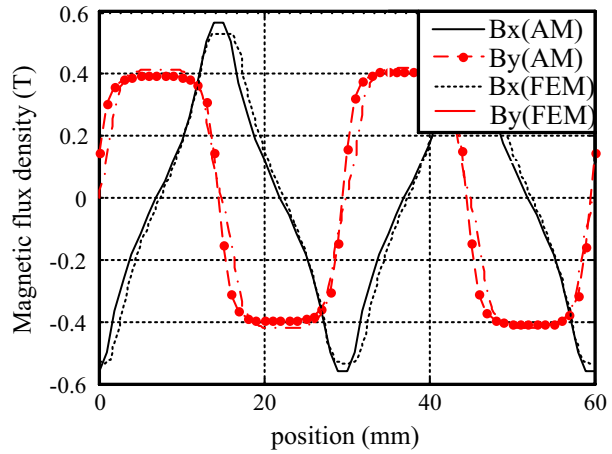

(a) Air-gap magnetic flux density

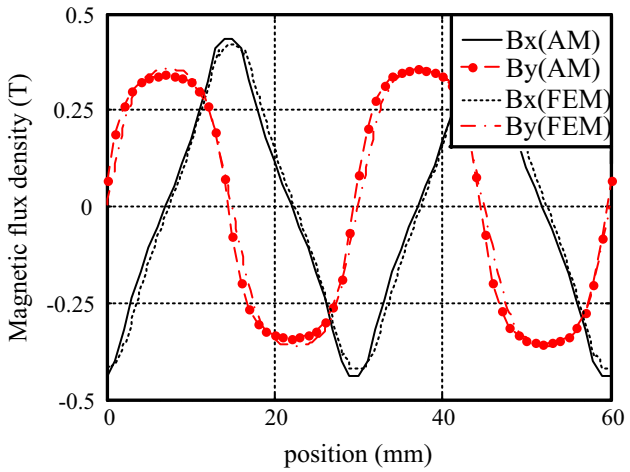

(b) Winding surface magnetic flux density

Fig. 10 Magnetic flux density of the SST-SPMLSM

tangential magnetic flux densities of the SST-SPMLSM are 4.70% and 4.19% higher than that of the FEM, respectively. However, the AM is used to calculate the air-gap and winding surface maximum radial magnetic flux densities of the SST-SPMLSM are 2.10% and 1.03% lesser than that of the FEM, respectively. From the results, it satisfies the design requirements of the SST-SPMLSM. In the meantime, the results also verify the availability and correctness of analytical method.

5.2 Detent Force

Detent force is the sum of the interaction between the tooth groove and the PM and the interaction between the ferromagnetic end and the PM. Then, the detent force of the interaction between the tooth groove and the PM is the main detent force of the electric machine. The detent force of electric machine causes thrust force fluctuation, vibration and speed control degradation, so appropriate methods should be adopted to reduce the detent force. Due to no groove of the SST-SPMLSM, there is no interaction force between the tooth groove and the PM. Therefore, the detent force of the SST-SPMLSM is very small.

The detent force of the SST-SPMLSM is analyzed and calculated, and the results are displayed in Fig. 11. It is found that the detent force of the electric machine with two ends is higher than that of middle part because of the primary and secondary yoke end disconnected and winding distribution unbalanced of the SST-SPMLSM. Through the analysis of the results, the detent force is 0.73% of electromagnetic thrust force in the electric machine.

5.3 Electromagnetic Thrust Force and Vertical Force

The electromagnetic thrust force is one of the important performance indexes of electric machine. This paper is used the Maxwell's tension vector method to calculate the thrust

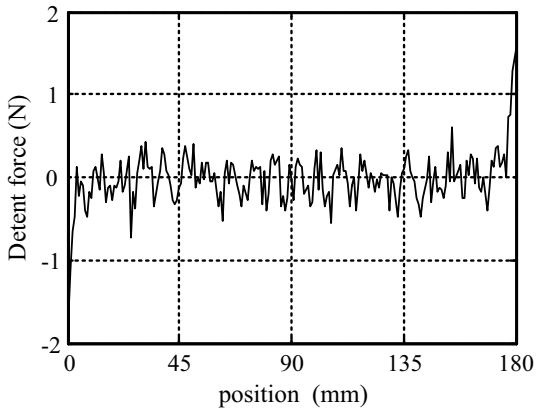

Fig. 11 Detent force

force of the SST-SPMLSM. The electromagnetic thrust force of electric machine is expressed as follow [15]

$$F_x = -\frac{2pl_{\delta 2}}{\mu_0}\int_0^{\tau} B_{x\delta av}B_{y\delta av}dx \tag{23}$$

where F_x expresses the electromagnetic thrust force, $l_{\delta 2}$ expresses the secondary transverse width, $B_{x\delta av}$ expresses the air-gap tangential average magnetic flux density, $B_{y\delta av}$ expresses the air-gap radial average magnetic flux density, and p expresses number of pole pairs.

The vertical force of electric machine is expressed

$$F_y = \frac{pl_{\delta 2}}{\mu_0}\int_0^{\tau} [(B_{x\delta av})^2 - (B_{y\delta av})^2]dx \tag{24}$$

where F_y expresses the vertical force.

The FEM is used to analyze and calculate the electromagnetic thrust force and vertical force of the SST-SPMLSM, which the results are shown in Fig. 12. It is found that the electromagnetic thrust force and vertical force of the SST-SPMLSM for the AM is 4.29% and 3.75% lesser than that of the FEM, respectively. Meanwhile, the electromagnetic thrust force of the SST-SPMLSM for the AM is 3.33% lesser than the rated thrust force. From the results, it satisfies the design requirements of electric machine, and also verifies the correctness and effectiveness of analytical method.

5.4 Static Force–Displacement Characteristic

Static force–displacement characteristic is one of the most basic characteristic of the electric machine, and also the basis of dynamic characteristic analysis for the electric machine. The paper refers to the static electromagnetic thrust force of the SST-SPMLSM under the secondary movement and primary winding DC current conditions.

The AM is used to analyze and calculate the thrust force of the SST-SPMLSM, and the results are illustrated in Fig. 13. It is found that the AM is used to solve the electromagnetic thrust force of the SST-SPMLSM is 4.62% lesser than that of the FEM. Meanwhile, the electromagnetic thrust force of the SST-SPMLSM is 3.23% lesser than the rated thrust force. Figure 13 shows the electromagnetic thrust force of the SST-SPMLSM with two ends to use the FEM is different of that of the SST-SPMLSM with middle because of primary and secondary yoke end disconnected and winding distribution unbalanced of electric machine. Then, the AM is used to calculate the same electromagnetic thrust force of the electric machine at ends and middle because of ignoring the influence of the above situation. From the result, it satisfies the requirements of the design SST-SPMLSM, and verifies the correctness and effectiveness of analytical method.

6 Conclusion

This paper mainly studies performance parameters of the short-secondary type slotless permanent magnet linear synchronous motor (SST-SPMLSM) based on the analytic method (AM). In order to improve the accuracy of analytical calculation, this paper proposes groove-by-groove method to analyze and calculate winding ECD. Meanwhile, the volume current density is used to equivalent the PM current density according to actual situation. In the meantime, the divided layers model of the SST-SPMLSM is built. On this basis, the magnetic flux density of each region in the SST-SPMLSM is solved. According to the electric machine structure and working principles, a 30 N SST-SPMLSM is designed. Based on the analytic hierarchical model and design dimensions of electric machine, the SST-SPMLSM is analyzed

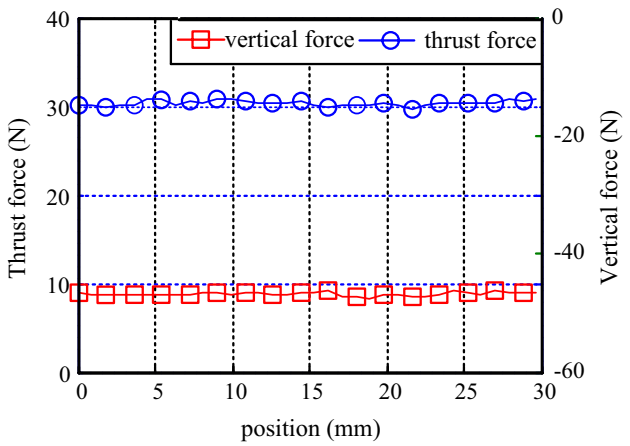

Fig. 12 Electromagnetic thrust force and vertical force

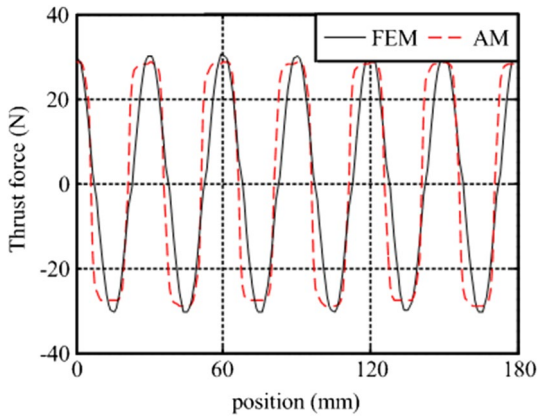

Fig. 13 Electromagnetic thrust force of the SPMLSM with different positions

and calculated, which is verified by the FEM. According to analysis of results, the following conclusions are obtained.

According to the actual situation, the groove-by-groove method and volume current method are used equivalent current density of the windings and PMs, respectively.

Based on the ECD and analytic hierarchical model of the electric machine, the magnetic flux density of each region in the SST-SPMLSM is solved by the separated variable method.

Through the parameters analysis of a 30 N SST-SPMLSM, the AM is used to solve air-gap and winding surface magnetic flux density curves of the SST-SPMLSM are basically the same with that of the FEM. Meanwhile, the electromagnetic thrust force of the SST-SPMLSM for the AM is 4.29% lesser than that of the FEM. From the results, it satisfies the design requirements of the electric machine, and also verify the correctness and effectiveness of analytic method.

Acknowledgements The authors want to thank the funding support from the Youth Backbone Fund of Henan University of Urban Construction with Grant Numbers G2015008.

Funding Youth Backbone Fund of Henan University of Urban Construction (No. G2015008).

Declarations

Conflict of interest The authors declare that they have no conflict of interest.

References

1. Yoshimura T, Kim HJ, Watada M et al (1995) Analysis of the reduction of detent force in a permanent magnet linear synchronous motor. IEEE Trans Magn 32(6):3728–3730
2. Liu C, Gao H, Xiong Y et al (2019) Detent force reduction in permanent magnet linear synchronous motor base on magnetic field similarity method. IEEE Access 7:57341–57348
3. Qinfen Lu, Bocheng Wu, Yao Y et al (2020) Analytical model of permanent magnet linear synchronous machines considering end effect and slotting effect. IEEE Trans Energy Convers 35(1):139–148
4. Park E, Jung S, Kim Y (2016) A design of optimal interval between armatures in long distance transportation PMLSM for end cogging force reduction. J Electr Eng Technology 11(2):361–366
5. Shin KH, Park HI, Kim KH, Jang SM, Choi JY (2017) Magnet pole shape design for reduction of thrust ripple of slotless permanent magnet linear synchronous motor with arc-shaped magnets considering end-effect based on analytical method. AIP Adv 7:056656
6. Kim M-Y, Kim Y-C, Kim G-T (2004) Design of slotless-type PMLSM for high power density using divided PM. IEEE Trans Magn 40(2):746–749
7. Kang G-H, Hong J-P, Kim G-T (2001) Design and analysis of slotless-type permanent magnet linear brushless motor by using equivalent magnetizing current. IEEE Trans Indu Appl 37(5):1241–1247
8. Zi-jiao Z, Mei-zhu L, Bao-quan K et al (2018) Characteristic analysis of a trilateral permanent magnet linear synchronous motor with slotless ring windings. IET Electr Syst Transp 8(1):20–26
9. Jang S-M, You D-J, Jang W-B et al (2005) Dynamic characteristics for position control of permanent magnet linear synchronous motor with control parameters. Proc Eighth Int Conf Electr Mach Syst 3:1893–1898
10. Ghaffari A, Rahideh A, Ghaffari H et al (2020) Comparison between 2-D and 0-D analytical models for slotless double-sided inner armature linear permanent magnet synchronous machines. Int Trans Electr Energy Syst 30(9):1–15
11. Huang XZ, Li J, Tan Q et al (2018) Design principles of a phase-shift modular slotless tubular permanent magnet linear synchronous motor with three sectional primaries and analysis of its detent force. IEEE Trans Ind Electron 65(12):9346–9355
12. Min SG, Sarlioglu B (2017) Analytical calculation of back EMF waveform for linear PM motors in slotted and slotless structures. IEEE Trans Magn 53(12):8112910
13. Kyung-Hun S, Kyong-Hwan K, Keyyong H (2017) Detent force minimization of permanent magnet linear synchronous machines using subdomain analytical method considering auxiliary teeth configuration. IEEE Trans Magn 53:1–4
14. Chen Li, Yuejin Z, Libing J (2013) Researches on an exact analytical method of halbach-array permanent-magnet motors with semi-closed slots. Proc CSEE 33:85–94
15. Rahideh A, Ghaffari A, Barzegar A et al (2018) Analytical model of slotless brushless PM linear motors considering different magnetization patterns. IEEE Trans Energy Convers 33(4):1797–1804

Hao Liu was born in 1981. He received the B.S. and M. S. degrees in Electrical Engineering from Henan Polytechnic University, Jiaozuo, China, in 2004 and 2007, respectively. He received the Ph.D. degrees in Electrical Engineering from Shenyang University of Technology, Shenyang, China, in 2020. Since 2007, he has been a teacher with School of Electrical and Control Engineering, Henan University of Urban Construction, Pingdingshan, China. His current research and teaching interests include electric machine and their control systems, and wind power generation. For the last several years, He has presided and participated in more than 10 scientific research projects, and composed 1 monograph, and published more than 40 papers in academic journals and international conference proceedings on electric machines and control systems, of which 10 were cited by SCI/EI.

Xiaoju Yin was born in 1974. He received the B.S. degrees in Computer Science from Liaoning University, Shenyang, China, in 1997. He received the M. S. degrees in Control Engineering from Shenyang University of Technology, Shenyang, China, in 2011. He received the Ph.D. degrees in Electrical Engineering from Shenyang University of Technology, Shenyang, China, in 2019. Since 2018, he has been an professor at the School of Renewable Energy Science and Engineering, Shenyang Institute of Engineering. Prof. Yin was selected as "Liaoning Province Hundred Million Talents Project" Hundred People Level, the 11th Liaoning Excellent Science and Technology Worker, the title of "Academic Goose" in Liaoning Province, Shenyang Leading Talents Title. His research and teaching interests include new energy power generation and its control technology.